DETechnologies Midterm Report
Memorial University of Newfoundland and Labrador
ME 8705 - Mechanical Engineering Capstone II

Miri, Shakib	Palmer, Logan	Clark, Aidan	Cleary, Patrick
smiri@mun.ca	lrpalmer@mun.ca	amhclark@mun.ca	pcleary@mun.ca
201848900	201906765	201919990	201901261

Team Supervisor:
Dr. Xili Duan
xduan@mun.ca

26 February 2024

Abstract

Improvements to traditional de agration engines are becoming harder to achieve, and there is a growing interest in longer-distance space exploration, so an energized research and development environment has grown revolving around detonation engines, particularly Rotating Detonation Engines as a potential propulsion advancement. Theoretical estimations of rotating detonation engine performance are up to 25% higher than performance seen in traditional de agration rocket engines. Through conducting a literature review, it has been discovered that there is a signi cant lack of publicly available literature detailing an in-depth design process of an RDE. DETechnologies aims to add information to that knowledge gap in the way of developing a complete analytical method to explicitly design an RDE.

Preliminary design work builds an analytical model that aims to predict the thermo-chemical and performance metrics of an RDE. Using parameters obtained from the analytical model, numerical simulation in Computational Fluid Dynamics and Finite Element Analysis will be conducted to ensure the rotating detonation engine will perform as expected while maintaining safe operation.

Flow systems and data acquisition techniques are also considered to increase the robustness of the design, and the possibility of creating an experimental prototype for further design validation.

Contents

List of Figures

List of Tables

1 Introduction and Background

1.1 Topic Introduction

A Rotating Detonation Engine (RDE) is a novel engine operating on the principle of detonation, meaning supersonic combustion. Detonation is a highly e cient mode of combustion with applications in astronautical, aeronautical, and defence industries. Peak theoretical e ciencies of detonation combustion compared to traditional sub-sonic combustion ranges between 10% and 25% [1]. While detonation engine technology is very immature, existing only in the research industry, harnessing the power of detonation is not a new concept. Early groundwork for a RDE was established by Voitsekhovskii in 1959 [2] with a continuous gas detonation process in a toroidal combustion chamber [3]. Since the 1950s, there has been some interest in detonation engines, but the research sector has not taken o until the past 10 years. Advancements in traditional de agration engines are slowing, along with a renewed interest in space exploration, the aerospace sector has begun looking at detonation engines as a potential option.

Via this capstone project, the DETechnologies team is seeking to learn more about detonation theory and to better understand the bleeding edge of propulsion engine technology, to satisfy our interests. The technical goal for this project is to ll the identi ed gap of a not-well-explored design process, by designing a small-scale gaseous Hydrogen/Oxygen propellant RDE capable of theoretically producing 1350N of thrust.

1.2 Current Progress

1.2.1 Problem De nition

There currently exists very little publicly available literature that explicitly summarizes the design process for sizing a small scale, research purpose RDE. Some publications that do outline some elements of the basic RDE design progress are Connolly-Boutin [4], Mundt [5], and Zhdan outlining the process of modelling combustion in GH_x=GO_x [6], however each step in the design process is not well de ned throughout the industry, owing to the immature nature of the technology. The design process of any thrust-producing engine requires modelling tools and a process to develop performance metrics and design points that can achieve an application. The DETechnologies team will go through the exercise of sizing a small scale RDE based on existing literature, including experimental data and rst-principles detonation theory.

1.2.2 Alternate Solutions

RDEs have only been utilized in the research industry to study the rotating detonation phenomenon, owing to the immature state of the technology. To explore RDE operation, two main approaches are often taken to build a successful engine: 1) trial and error, and 2) proven engine basis.

The rst alternate approach, the trial and error method, is a brute force, cost-intensive approach. This approach involves building several engines of varying sizes based on rudimentary calculations. Engines are tested with all accessible propellants at various input temperatures, pressures, equivalence ratios, and mass ow rates until detonation is achieved. The Bykovskii rules of thumb for minimum geometry for RDE uses a similar approach [7]. Fotia [8] and Kindracki [9] take similar, brute force experimental approaches [8].

The second alternate approach, is well apt for research projects interested in studying small variations in operational parameters, or investigations of combustion propagation phenomena. This method does not concern itself with validation of design process, rather a plug and play approach.

Both of these approaches are not realistic for a capstone project and require signi cant time and knowledge regarding explosives testing. Hence the chosen approach of attempting to implementing rst-principles detonation theory, coupled with minimum viable engine rules. This approach allows a minimum viable engine to be designed from scratch, and compared to published experimental data. Parameters can largely be validated without experimental testing. Many research institutions opt for this approach for full control and understanding of the mechanics involved [4].

1.2.3 Constraints

Some constraints identi ed that are driving the design process for this engine are summarized in Table 1.

Table 1: Summary of Major Constraints

Technical	Costs	Safety	Timeline
• No local knowledge of detonation. • No local knowledge of supersonic uid ow, or compressible uids.	• Capstone group budget of $ 250 cost matching with the faculty. Student contributions must make up the rest .	• No combustion testing facilities in the region. • No team experience handling or designing GH/GO systems.	• Only 2 months remaining until graduation.

1.3 Literature Review

Harnessing the power of detonation makes RDEs signi cantly more e cient, with estimates of 25% higher fuel e ciency than traditional de agration rocket engines [10]. The background theory and focus of the theoretical engine designed by DETechnologies will focus on H2-O2 detonation reactions and preexisting RDEs. Most combustion engines can be approximated by the Brayton cycle, an isobaric combustion process. Detonation combustion cycles are approximated by the Humphrey or Fickett-Jacobs cycles. The Humphrey cycle is an ideal isochoric, or pressure gain, combustion cycle, whereas the Fickett-Jacobs cycle is a similar, pressure gain combustion cycle, modeled to more closely represent the physical detonation process. E ciency gains of isochoric combustion cycles compared to isobaric combustion are easily seen from their respective Pressure-Volume (PV) curves. PV curves of Brayton (isobaric), Humphrey (isochoric), and Fickett-Jacobs (isochoric) cycles are shown in Figure 1.

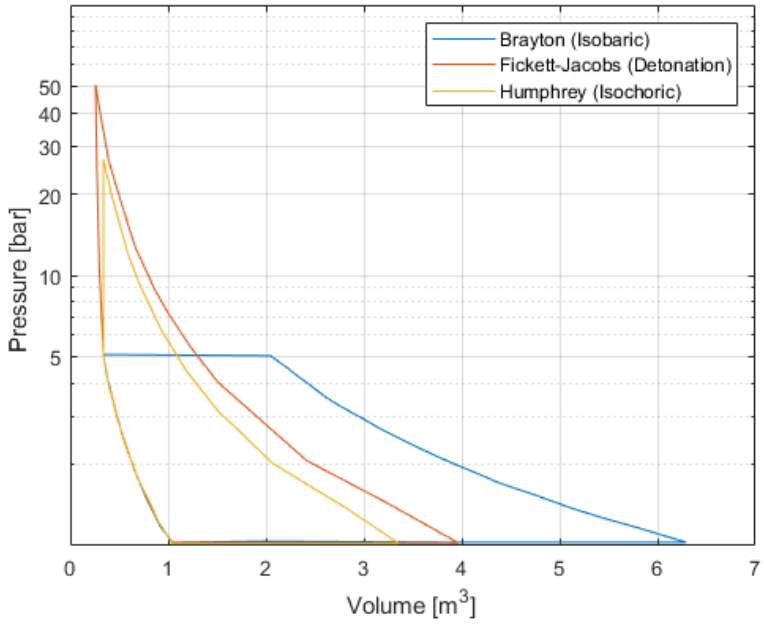

Figure 1: PV Diagram for Brayton, Humphrey, Fickett-Jacobs Cycles, adapted from Wolanski [11]

In each of the four cycles depicted in Figure 1, the process between each numerical state can be generalized as follows.

- 1 ! 2 : Compression.
- 2 ! 3 : Combustion.
- 3 ! 4 : Expansion.
- 4 ! 1 : Compression (via cooling).

The di erence between Isochoric and Isobaric combustion is shown in the combustion stages between states $2 \rightarrow 3$. Notice the constant pressure line between states 2 and 3 of the Brayton cycle, compared to the constant volume process between states 2 and 3' and 3" of the Humphrey and Fickett-Jacobs cycles, respectively. Since the area under the PV curve is representative of the e - ciency of the cycle, it is straightforward to visually see how the high peak of the isochoric combustion cycles contributes to the overall higher e ciency of detonation cycles. Theoretical cycle e ciencies for stoichiometric combustion of hydrogen and air for each of these three cycles are shown in Table 1 according to [1].

Table 2: Combustion Cycle E ciencies for Stoichiometric Combustion Between Hydrogen and Air [1]

Reactants		Brayton [%]	Humphrey [%]	Fickett-Jacobs [%]
Hydrogen & Air at	=1.00	36.9	54.3	59.3

There are two main types of detonation engines; the Pulse Detonation Engine (PDE) and the continuous detonation engine. Pulse Detonation Engines operate cyclically in a ll, re, purge cycle. The e ciency of these engines is limited by the upper frequency at which this three-stage cycle can occur. Continuous detonation engines, alternatively known as Rotating Detonation Engine (RDE)s, are not burdened by a cyclic, mechanically driven, combustion process. As the names suggest, continuous detonation engines operate such that a combustion wave continually propagates through the combustion chamber while fresh propellant is continually injected.

The early groundwork for an RDE was established by Voitsekhovskii in 1959 [2] with a continuous gas detonation process in a toroidal combustion chamber [12]. Since then, a handful of groups have investigated detonation engines, with increased attention in the last ten years. The increased attention is primarily due to the e ciency gains these engines can o er, and the global focus/need on greener and faster ight. The rst widely accepted theory which attempts to describe detonation combustion is the Chapman-Jouguet (CJ) theory, which is a synthesis of Chapman [13] and Jouguet [14] zero-th dimensional approximation of properties across a detonation wave front. These theories attempt to describe the relation between thermo-chemical properties of reactants and products across a detonation wave. Kuo [10] presents a full derivation of the Rankine-Hugoniot relation from the conservation equations shown in Equations 1 through 3 [10]. The Hugoniot relation, shown in Equation 4, describes the solutions for all downstream pressure, p_2 and speci c volume, $= \frac{1}{2}$, given initial conditions p_1, $_1$ ^{1} and heat of combustion q_{rxn}, if chemical reaction is present.

Continuity.

$$\frac{d(u)}{dx} = 0 \tag{1}$$

Momentum.

$$u\frac{du}{dx} = \frac{dp}{dx} + \frac{d}{dx}[(\frac{4}{3} + {}^{0})\frac{du}{dx}] \tag{2}$$

Energy.

$$u[\frac{d}{dx}(h + \frac{u^2}{2})] = \frac{d}{dx}q_{cond} + \frac{d}{dx}[u(\frac{4}{3} + {}^{0})\frac{du}{dx}] \tag{3}$$

$$\frac{}{1}(\frac{p_2}{_2} - \frac{p_1}{_1}) - \frac{1}{2}(p_2 - p_1)(\frac{1}{_1} + \frac{1}{_2}) = q_{rxn} \tag{4}$$

Where is the ratio of reactant speci c heats.

Two critical points identi ed by the CJ theory are called the upper and lower CJ points, respectively [13][14]. The upper and lower CJ points represent the minimum and maximum points where detonation

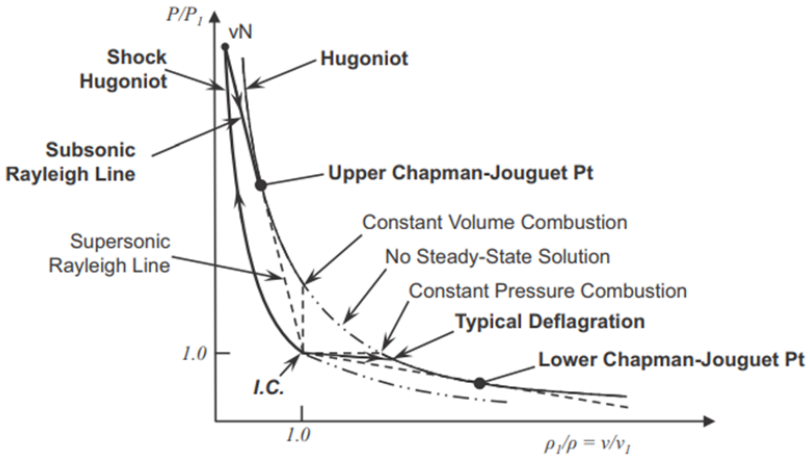

Figure 2: P-V Diagram of Rankine-Hugoniot Curves [15]

and de agration can exist, respectively. Figure 2 described in detail the relation of the CJ points to detonation and de agration [15]. Understanding where and how the CJ points can be in uenced is essential in designing a combustion system to behave as expected, as they are representative of the physical operating conditions in a system.

The Hugoniot curve can be divided into ve regions, as shown in Figure 3, where each region represents a di erent combustion mode. Not all of these combustion modes are physically realizable. Regions of particular interest are I - Strong Detonation and II - Weak Detonation, divided by the upper-Chapman-Jouguet (UCJ) point. The UCJ point is de ned by the position at which a line drawn from P_1, $_1{}^1$ (the Rayleigh Line) is tangent to the Hugoniot curve.

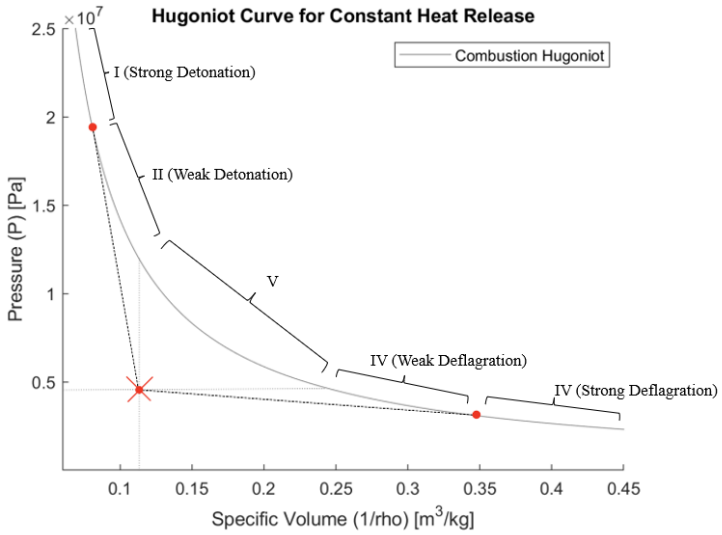

Figure 3: Combustion Regions represented on Hugoniot plot adapted from Kuo [10]

In region I - Strong Detonation, it can be shown that the pressure of the post-combustion gasses is higher than the pressure of the combustion wave itself, $P_2 > P_C$. The detonation wave travels below the speed of sound in this region [10]. This type of detonation is hard to achieve, requiring extreme con nement [10]. Region II - Weak Detonation has a bi-product pressure less than the pressure of the combustion wave $P_2 < P_C$. Gas speed in this region slows down signi cantly across the combustion

wave but still remains above the speed of sound [10]. Weak detonation requires reactants with very high-speed chemical kinetics [10]. The point of speci c interest in the design of RDEs is the Upper-CJ point, where combustion bi-products maintain the same pressure as the combustion wave and travel at the speed of sound in the burned gas mixture. The CJ is also the local minima of entropy generation [16]. Because of this minimum of entropy, and the di cult requirements needed to achieve states 1 and 2, if detonation is instigated within states 1 and 2, it will tend towards the Upper CJ point [17].

The Zel'dovich, von Neumann, and Doring (ZND) theory is built upon the Chapman Jouguet theory by Zel'dovich [18], von Neumann [19] and Doring [20]. These theories extend CJ theory by considering the combustion wave as 1D and steady relative to the detonation front. These theories collectively postulate that a detonation wave consists of a leading shock wave that compresses the reactants, thereby increasing the pressure and temperature, followed by a secondary chemical reaction, a combustion wave. The zone in between the leading shock and combustion wave has been termed the induction zone, and no chemical reactions occur. According to these theories, the leading supersonic shock wave compresses the reactants such that the following combustion wave propagates at a subsonic speed relative to the reactants but at a supersonic speed relative to a pre-compression reference frame. The temperature increase from the compression also increases the thermal e ciency of combustion, due to resultant higher combustion temperatures. A ZND representative detonation wave is shown by Kuo [10] in Figure 4.

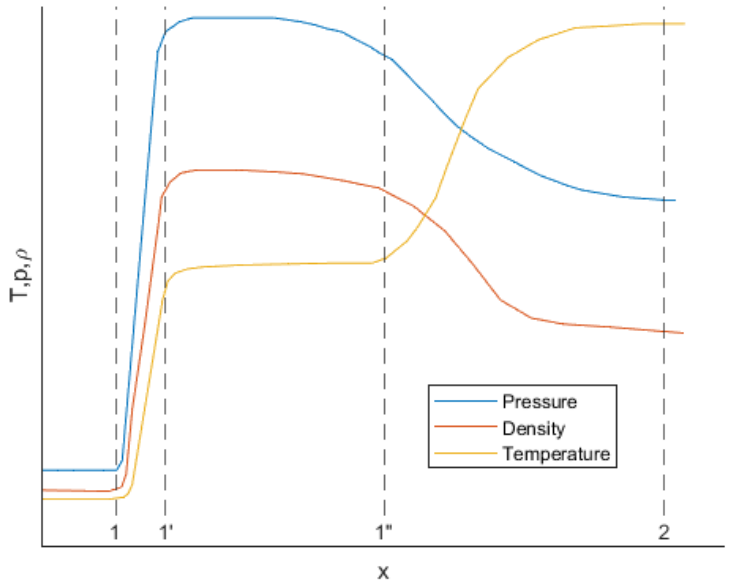

Figure 4: ZND Wave Structure Adapted from Kuo [10]

Figure 4 shows four key points of Temperature T, Pressure P, and Density . Initial properties increase steeply across the width of the leading shock wave from point 1 to 1'. Position 1' is also called the von Neumann spike, the point at which the system reaches its maximum pressure. Within the induction zone, between states 1' and 1", the pressure, temperature, and density all remain roughly constant at the compressed state. At point 1", the mixture reacts; pressure P and density drop, while temperature T increases sharply. As discussed earlier, the decreased product pressure is still higher than the initial reactant pressure, hence the term pressure-gain combustion.

Geometric parameters of the RDE can be estimated using detonation cell size, , estimates based on [21], [22], [23]. Geometric engine parameters are estimated using rules of thumb from [1], [7], [24], and [25] correlated to detonation cell size estimates, summarized in Table 3.

Table 3: Summary of published Rules of Thumb for RDE Geometry According to Respective Theories

Parameter	Bykovskii [7]	Nair [25]
Minimum Fill Height, h	(12 5)	N/A
Minimum Outer Diameter, D_{min}	28	40
Minimum Channel Width, $_{min}$	$\frac{h}{5}$	2:4
Minimum Length, L_{min}	$> 2h$	24

A well-used engine with a substantial publication series is a non-premixed, Hydrogen-Oxygen RDE built and tested by Zucrow Laboratories at Purdue University, Air Force Research Laboratory (AFRL) [26], Air Force Institute of Technology (AFIT) [16], University of Central Florida (UCF) [27], and the University of Washington (UW) [5]. Mundt [5] provides detailed design information for this RDE. This engine was built with the objective of increasing consistency and comparability between functioning RDE experimental data [26].

In order to have a direction and form of achievable validation for the analytical model being developed, this experimental RDE's theoretical performance has been selected as the design point. The intent is to use the analytical model to generate engine speci cations that theoretically produce 1350N of thrust, and is within 25% of the stated thermo-chemical and geometric parameters.

1.4 Patent Search

Details of two United States patents are summarized in the following sections. These two patents are selected as the described products are very well-detailed, and closely resemble the end product for this Capstone project. Additional relevant patent summaries can be found in Appendix A.

1.4.1 Detonation Rocket Engine Comprising an Aerospike Nozzle and Centring Elements with Cooling Channels

The United States patent US 11,795,891 B2 [28] is entitled "Detonation Rocket Engine Comprising an Aerospike Nozzle and Centring Elements with Cooling Channels" and was published by Piotr Wolanski.

The patent comprises an annular detonation chamber with an aerospike, following a typical RDE design. The following is a summary of the claims made in the patent ling:

1. The detonation rocket engine comprises an annular chamber, Aerospike nozzle, with plumbing to connect propellant.
2. The detonation rocket engine is characterized so the Aerospike cooling nozzles is connected to one of the propellant supply lines.
3. The centering elements of the detonation rocket engine are streamlined.
4. The attached Aerospike has a truncated conical shape
5. The detonation rocket engine has an annular combustion chamber and connected nozzle which can adapt to external conditions. In addition to this, there are at least three evenly distributed centering elements between the inner and outer walls.
6. The nozzle of the engine has additional cooling channels which are connected to propellant feed lines.
7. The centering elements of the engine have a streamlined shape.
8. The nozzle of the engine has a truncated conical shape.

1.4.2 Rotating Detonation Engine Injector and Method of Designing

The United States patent US 2023/030931 [27] is entitled "Rotating Detonation Engine Injector and Method of Designing" and was published by Robert Burke.

The patent comprises an injector plate design, speci c to a RDE developed by the University of Central Florida Research Foundation. A summary of the claims made in the patent ling are:

1. The patent covers the method of propellant injection discussing initial conditions for fuel and oxidizer ow into the engine, mass ow rate, and injector cross-sectional area, in addition to ideal pressure and temperature requirements.
2. Preferred engine fuel is hydrogen and oxidizer is oxygen.
3. The mass ow rate of the propellant is calculated by the identi cation of the fuel-air equivalence ratio and the mass ow rate of each respective propellant.
4. The mass ow rate is calculated based on previous used propellant ow rates in an RDE.
5. The temperature of each propellant is based on the propellant feed system of the RDE.
6. The upstream pressure of the propellants is determined by previous RDE feed systems.
7. Inadequate injection results in upstream and down stream de agration, quenching detonations and poor mixing of H2/O2 due to Hydrogen's high di usivity, low density, and high injection velocities.
8. Claim 1 further includes the calculation of the ideal total momentum of the engine and the momentum of each propellant. This data is used to adjust the mass ow rate if the momentum of the RDE does not meet an idealistic requirement.
9. Propellant injection design comprises identi cation of preferred fuel and oxidizer, initial mass ow rate, ideal temperature, and con guration to ensure required pressures can be obtained.
10. Claim 9 uses hydrogen as fuel and oxygen as oxidizer.
11. Calculation of mass ow rate requires the calculation of fuel-air equivalence ratio, total mass ow, and each propellant mass ow rate based on the equivalence ratio.
12. Propellant temperature is calculated based on propellant supply and storage.
13. Identi cation of ideal total momentum and actual total momentum of the RDE is required to accurately design an injector plate.
14. Based on the upstream pressure of fuel and oxidizer, select a pressure ratio in the range of 0.8775 - 1.4917.
15. Each fuel injector is paired with an oxidizer injector, such that the fuel-oxidizer pressure ratio is in the range of 0.8775 - 1.4917.
16. The injectors of the RDE use hydrogen as fuel, and oxygen as oxidizer.
17. Each injector pair is arranged in a doublet con guration with an interior angle between 55°and 65°.
18. The injector pairs are arranged in a circular pattern in the RDE combustion chamber.
19. The injector pairs are found in a radial direction by injector diameter between 2.5 - 2.7.
20. The injector pairs are found in a circumferential direction by injector diameter between 3.3 - 3.6.

2 Project Management

2.1 Task Division

As described in the Project Management Plan (PMP), the team has decided on a collaborative approach to task sharing. This allows for more brainstorming and better idea re nement to improve concepts. To ensure progress is made and no tasks get forgotten, each task is assigned to someone as the 'responsible party', ensuring that the task reaches completion on time. The tasks and team member assignments are summarized below in Table 4.

Table 4: Task Division Summary

Team Member	Main Task(s)
Shakib Miri	Analytical Model Development, Compressible Flow Modeling.
Logan Palmer	Analytical Model Development, Combustion CFD, Thrust Stand Design.
Aidan Clark	Structural Analysis, Numerical Simulations: CFD (combustion & propellant mixing), FEA (static, modal, fatigue).
Patrick Cleary	Detailed CAD, DFMA, Manufacturing Drawings with GD&T

These sub-tasks will only be discussed in detail in the methodology, and results sections. For a breakdown on the sub-tasks within these sub-tasks, please see previously submitted PMP.

2.2 Meeting Schedule

As described previously in the PMP, submitted on February 02, 2024, the DETechnologies team meets three times per week in addition to a time slot reserved for 'as-needed' meetings/working sessions. The meeting schedule is outlined in Table 5.

Table 5: Regularly Scheduled Meetings.

Meeting Description	Occurrence
Dr. Duan Update Meeting	Bi-weekly: Wednesdays at 12 (noon)
Group Working Session	Weekly: Mondays from 2pm-5pm
End of Week Update Meeting	Weekly: Fridays from 3pm-4pm
As-needed working session	As-needed: Wednesday 1pm-5pm.

2.3 Timeline

The initial planned timeline for the project for this four-month term was presented in the PMP submitted on February 02, 2024. Over the last three weeks, changes have been made to the timeline to accommodate prolonged task completion time. Each task has seen progression toward completion, however continual changes to the analytical model to create a more accurate design point have resulted in the need to extend detailed design tasks to incorporate these changes.

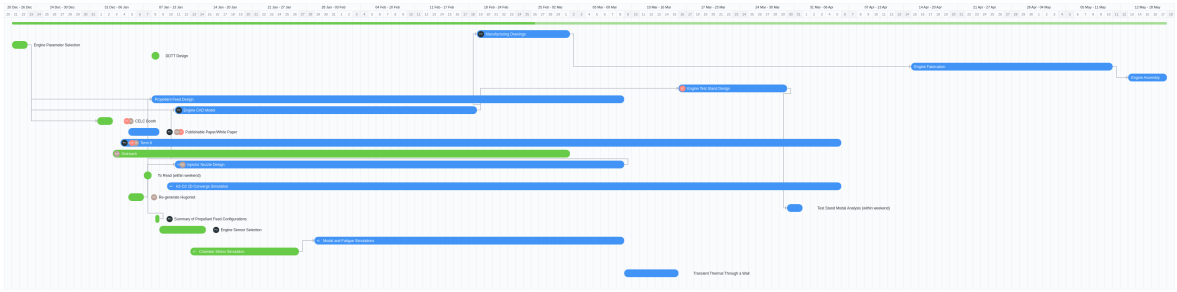

Figure 5: Updated Project Gantt Chart to re ect current statuses of project progress.

2.4 Deliverables

Summarizing the table of expected deliverables and the DETechnologies team's commitment to each of these deliverables is shown below in Table 6, as was shown in the original PMP submission.

Table 6: Summary of Deliverables and Objectives

Deliverable	Sub-Deliverable (where applicable)	Commitment Level
Analytical Model	Implementation of detonation theories to predict detonation parameters	Required
	Implementing empirical rules, and experimental data to size engine based on project constraints	Required
CFD Validation	Geometry de nition	Required
	Chemistry de nition and analysis	Not Required
Structural Analysis	Basic hand calculations	Required
	Finite Element Analysis (FEA) validation: Modal, Thermal, Stress Analysis	Required
Final Design	General geometry: both uid and structural considerations	Required
	Design for Manufacturing and Assembly	Required
	Sensor Integration	Required
Manufacturing	N/A	Not Required

3 Methodology and Initial Results

The rst two sub-sections in this section are simply to satisfy rubric items as prescribed by the MUN Mechanical Engineering Academic Term 8 Capstone project, which is designed for single term capstone projects. As this is a two-term capstone project, this information has been reported in Academic Term 7, and is largely paraphrased from previously submitted reports, using correct references where applicable. The nal report written for Academic Term 7 is the primary source of information for these sections [29]. The third sub-section and all subsequent sub-sub-sections provide an accurate, up-to-date review of the current project status.

3.1 Conceptual Design

The following concept generation is based on preliminary design work conducted in February through April 2023. It needs to be understood that we are much too far along in this project for this section to be a relevant deliverable. Early conceptual design work was *nished* over a year ago. Looking back at this initial scope clari cation, the conceptual design phase is not a valuable exercise at this point.

The overarching project goal chosen drastically reduces project scope into a very niche eld, however the following morphological chart in Table 7 will further reduce scope [29].

Table 7: Summary of conceptual design possible solutions to key features, borrowed from Miri et al. [29]

Feature	Solution 1	Solution 2
Initiation	Injection of pre-formed shock wave	Internal sparking
Continuous Detonation	Cylindrical combustion chamber	Non-circular (curved) combustion chamber
Injection Direction	Axial	Axial + Radial
Injection Scheme	Pre-mixed	Non-pre-mixed
Propellant	Gas	Liquid
Exhaust Outlet	Blunt	Nozzle

According to the discussions presented by Miri et al. [29], choices that are made to reduce this morphological chart from 2 potential solutions to 1 are based on the probability of increasing hot- re success, and to a lesser extent the mechanical complexity of solution implementation. A summary of the chosen baseline solution and reasoning is presented in Table 8 [29]. Additional details on the reasoning for the choices made are elaborated on in Sections 2 and 3 of Miri et al. [29].

Table 8: Summary of chosen conceptual design, adapted from Miri et al. [29]

Feature	Solution	Reasoning
Detonation Initiation	Injection of pre-formed shock wave	Increased chance of successful initiation of detonation wave.
Continuous Detonation	Circular combustion chamber	Decreased mechanical complexity, and increasing probability of sustaining a detonation wave with lesser troubleshooting.
Injection Direction	Axial	Simpler mechanical design.
Injection Scheme	Non-pre-mixed	Less dangerous than working with a pre-mixed explosive mixture.
Propellant	Gas	Ease of accessibility.
Exhaust Outlet	Nozzle	Increasing thrust output of engine.

As will be noted later in this paper, the exhaust outlet: nozzle was scrapped in the year between originally writing this due to high complexity that does not align well with the core value of the project, which is to design a functional RDE.

3.2 Preliminary Design

This section is broken down into the major sub-sections of this project: Analytical Model, Computational Fluid Dynamics (CFD), Structural Analysis, Data Collection, Propellant Supply System, and Design For Manufacturing and Assembly (DFMA). This section provides context and analysis of the current state of design work.

3.2.1 Analytical Model

3.2.1.1 Detonation Cell Size Predictions

An accurate detonation cell size prediction is important because critical engine geometry rules of thumb are based on the detonation cell size, as shown in Table 3. Four methods for predicting detonation cell size are implemented for this work; Westbrook [23], Gavrikov [21], Ng et al. [22], and SeanCB [30]. To validate the prediction methods, and to ensure they are implemented correctly, predictions are compared to experimentally obtained cell sizes from the California Institute of Technology (CalTech) detonation database [31]. Cell size predictions are plotted for a stoichiometric combustion reaction between Hydrogen and Oxygen at and T_0 = 293K, between 50 kPa < P_0 < 1000 kPa in Figure 6.

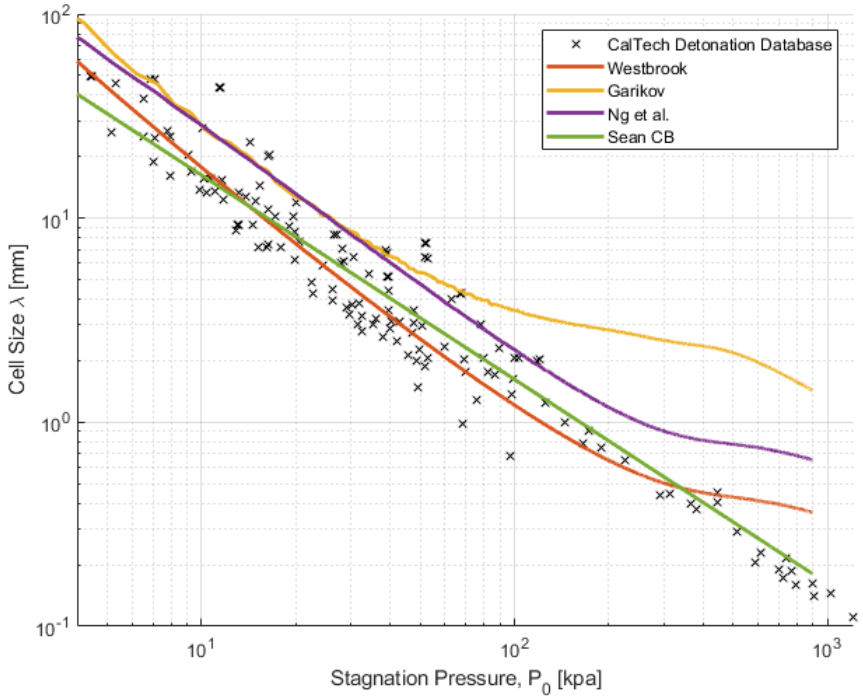

Figure 6: Theoretical and Experimental Detonation Cell Sizes for Hydrogen, Oxygen Combustion at $T_0 = 293K$, = 1:00 and 50 kPa < P_0 < 1000 MPa [31].

Figure 6 shows good agreement between the detonation cell size predictions and experimental results. All methods align well with experimental results at low stagnation pressures but diverge from experimental results at various points between 70 kPa (Garikov) and 450 kPa (Westbrook). It should be noted that successfully applying the Gavrikov correlation is challenging due to its reliance on activation energy. It is also interesting to note the similar behaviour between the Ng and Westbrook correlations, with the Ng estimating towards the higher end of the experimental cell size range, while Westbrook tends towards the mid-range of the data. Investigating the derivations and formula for Westbook and Ng, it is not obvious to see where the similar, but o set, behaviour comes from [23][22]. Connolly-Boutin [30] empirical correlation provides by far the best t to experimental data and will be used for further calculations regarding detonation cell size. This correlation was developed as an interpolation and curve t between the data presented in the Detonation Database [31].

To understand the cell size sensitivity to initial conditions, plots of detonation cell size versus both stagnation pressure and initial temperature are created, and shown in Figure 7.

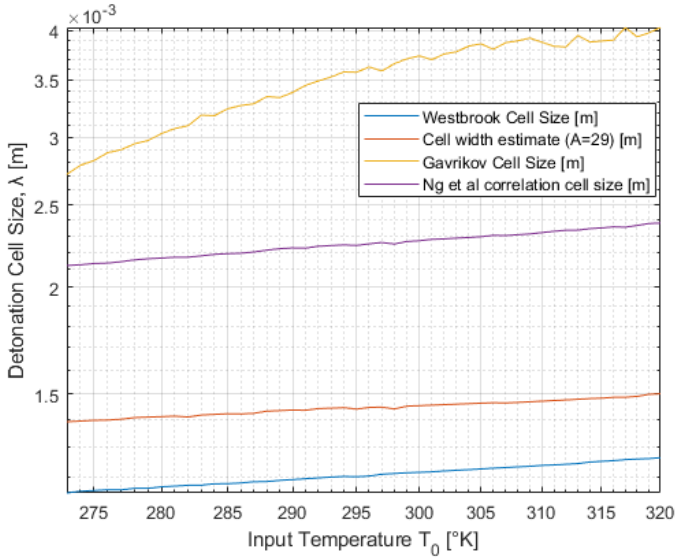

(a) Detonation Cell Size, λ, where $270K < T_0 < 320K$, P_0=101.325 kPa, ϕ=1

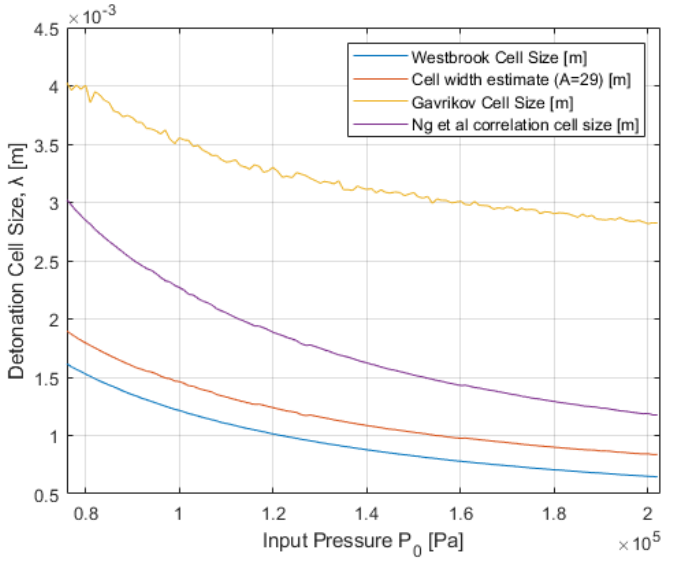

(b) Detonation Cell Size, λ, where 80 kPa $< P_0 <$ 200 kPa, T_0=293K, ϕ=1

Figure 7: Detonation Cell Size, Varying Input Parameters, T_0 & P_0

Figure 7a shows that the detonation cell size prediction is not very sensitive to changes in the initial temperature of the propellant, as detonation cell size predictions vary by 0.1mm across the 45K temperature range. On the other hand, Figure 7b shows that the detonation cell size is very sensitive to changes in the stagnation pressure (initial pressure) of the propellant, as the cell size prediction decreases by more than 1mm across the 80 kPa < P_0 < 300 kPa stagnation pressure range.

The third parameter that has the potential to in uence the detonation cell size, is the equivalence ratio, , a measure of how rich (> 1) or how lean (< 1) the propellant mixture is. The equivalence ratio is varied across a range, shown in Figure 8.

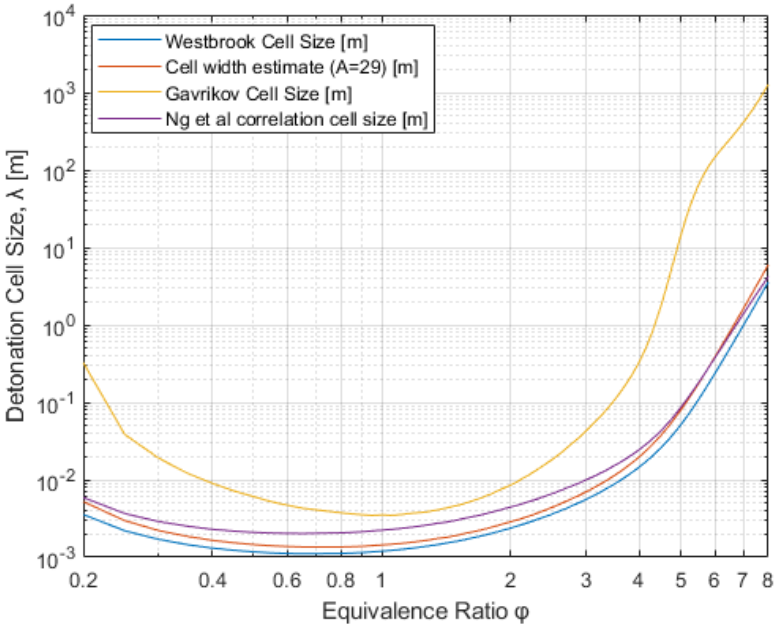

Figure 8: Detonation Cell Size Estimates Varying Input Equivalence Ratio , holding P_0=101.325kPa, T_0=293K.

As seen from Figure 8, detonation is very sensitive to variations in the equivalence ratio, as cell sizes range by 1 mm across a 0:5 of the propellant mixture.

3.2.1.2 Theoretical Thrust Considering an engine operating on perfect stoichiometric combustion, equivalence ratio = 1:00. Initial temperature has a negligible e ect on detonation cell size in comparison to stagnation pressure, therefore thrust output versus stagnation pressure can be used as the driving parameter to select the operating point.

Relating CJ and ZND detonation wave parameters to engine thrust is accomplished by approximating purely mean axial ow from a 2D azimuthal expansion process, as presented by Shepherd in [32]. Using a control volume approach, the net mean azimuthal ow at the exit of the combustion chamber is shown to be zero according to the conservation of angular momentum, evident by Equation 5 [32].

Conservation of angular momentum, M for stationary control volume and control surface @ [32].

$$M = \frac{@}{@t} \int r \quad u dV + \int_{@} (r \quad u) n \quad u dS \tag{5}$$

Where is density, r is the radius, and u is the velocity vector. Since the control volume surrounding the RDE does not rotate, the rst term evaluates to zero [32]. The second term can be re-written considering the geometry of a RDE, a simple annulus cylinder, assuming uniform ow in the radial direction, Equation 6 [32].

$$\frac{1}{2} \int_0^2 ({}^0; z) \ ({}^0; z) w({}^0; z) d \ {}^0 = \overline{w} = 0 \tag{6}$$

Where v is azimuthal speed, w is axial speed, is angle. The average of the azimuthal and axial, accompanied by the net-zero angular momentum indicates that $\overline{} << \overline{w}$ [32].

This understanding that pure azimuthal detonation ow within the combustion chamber of a RDE resolving to mean pure axial ow exiting the combustion chamber, allows for speci c thrust to be written. For the case of expansion to atmospheric pressure P_a and assuming isentropic expansion along streamlines, Equation 7 is written [32]. Full derivation of speci c thrust equation shown by Shepherd [32].

$$\overline{M}_{P_a} = w = a_1 \sqrt{\frac{2}{1}\left(1 + \frac{1}{2(\quad + 1)} M_{CJ}\right)^{2}} \left(\frac{1}{M_{CJ}}\right)^{\quad} \left(\frac{P_a}{P_1}\right)^{\frac{\quad}{\quad}} \sqrt{\frac{1}{M_{CJ}^2} \frac{\quad + 1}{M_{CJ}^2 + 1}^{\frac{\quad}{(\quad + 1)}}} \tag{7}$$

Where P_1 is the initial pressure, P_a is atmospheric pressure, is the ratio of speci c heats, M_{CJ} is the CJ wave Mach number. Using CJ detonating wave parameter, the resulting speci c thrust can be calculated, allowing detonation wave parameters to be related to RDE performance.

Mass ow rate $\dot{m}$ is calculated by considering the ll volume of the combustion chamber, de ned by combustion chamber geometry calculations as discussed in Section 3.2.1.3, and the time between subsequent waves in which injectors are not blocked. Mass ow rate calculation is summarized by Equation 8.

$$\dot{m} = h \quad V_{CJ} \tag{8}$$

Where h is critical ll height, is channel width; alternatively $= \frac{1}{2}(OD \quad ID)$ where OD - Outer Diameter, ID - Inner Diameter. is density, and V_{CJ} is the velocity of the detonation wave. As this is a theoretical equation, consistent units are su cient. According to the outlined process, thrust is plotted as seen in Figure 9.

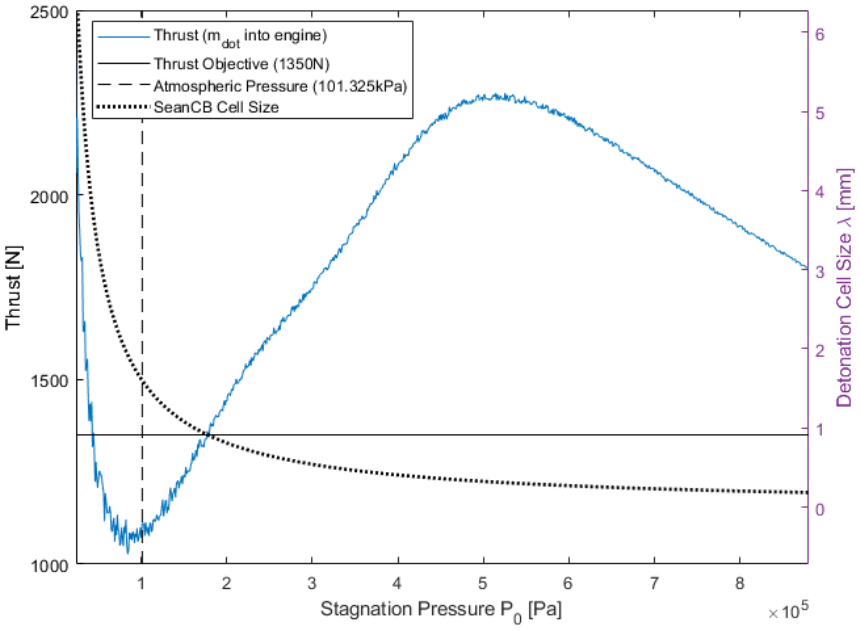

Figure 9: Thrust Versus Stagnation Pressure at = 1:00 and $T_0 = 293K$

From Figure 9, the intersection point between thrust objective and actual thrust can be read at a stagnation pressure of 180 kPa. The detonation cell size, according to Connolly-Boutin [30] is read as = 0:92 mm.

3.2.1.3 Engine Geometry With the value of = 0:92, the correlations presented in Table 3 can be used to determine a minimum engine size that would theoretically give us the performance required.

Selecting a design according to these ranges is an arbitrary process. To increase the probability of a successful engine, the high-end of these minimum ranges is selected. Maximizing the minimum geometry allows for a geometry that is minimized while surpassing all minimum rules of thumb. Given

this thought process, the correlations presented by Nair result in the largest engine geometry, therefore geometry calculated using the Nair correlations was selected.

Important engine parameters and operational points of interest are summarized below in Table 9.

Table 9: Summary of Selected Parameters

Parameter	Value
Stagnation Pressure, P_0	180 kPa
Initial Temperature, T_0	300 K
Equivalence Ratio,	1.00
Detonation Cell Size,	0.92 mm
Minimum Fill Height, h	15.64 mm
Min. Outer Diameter D_{min}	36.8 mm
Min. Channel Width $_{min}$	3.128 mm
Min. Length L_{min}	31.28 mm
Mass Flow Rate, m_{dot}	$32{:}8\frac{g}{s} < \dot{m} < 65{:}1\frac{g}{s}$
Peak Pressure, P_{VN}	6.03 MPa
Peak Temperature, P_{CJ}	3783 K
Wave Speed	2.866 $\frac{km}{s}$
Speci c Impulse, I_{SP}	414.7 s^{1}
Wave Number (Wolanski)	2

It needs to be understood that Table 9 presents *newly* discovered engine geometry parameters. Previously completed analysis used an analysis approach that was proven to be inaccurate for this situation. Results have been selected from this previous approach for some time now, and are still being used as the basis for continued work for the sake of this capstone project. Should any experimental work be conducted on this engine, the analysis conducted in the following paragraphs should be repeated given the updated engine parameters shown in Table 9. The old, not-as-accurate engine parameters that are used for continued analysis are shown below in Table 10 with most of the details removed to avoid potential confusion.

Table 10: Old Less Accurate Analysis Engine Geometry

Parameter	Value
Stagnation Pressure, P_0	130 kPa
Initial Temperature, T_0	300 K
Equivalence Ratio,	1.00
Detonation Cell Size,	1.621 mm
Minimum Fill Height, h	27.5 mm
Min. Outer Diameter D_{min}	55.1 mm
Min. Channel Width $_{min}$	4.7 mm
Min. Length L_{min}	47.0 mm

3.2.2 Computational Fluid Dynamics

Computational Fluid Dynamics for this engine takes many forms and will be an important step in predicting performance. CFD of the thermodynamics will take place in CONVERGE CFD, using a model provided in collaboration between Convergent Science and DETechnologies for an "unrolled" RDE two-dimensional model using air-hydrogen propellant [33]. DETechnologies uses this model as a baseline, as the propellant and geometry are altered to match the design selected using the analytical model.

In addition to the combustion simulations, CFD will also be used to conduct ow analysis to validate the double-choke ow problem faced while feeding the engine. In addition to validating the choked ow conditions, this ow simulation will also be used to analyze the mixing in the combustion chamber between the oxygen and hydrogen propellant feeds. The entirety of this portion of the CFD will be conducted using Ansys Fluent software.

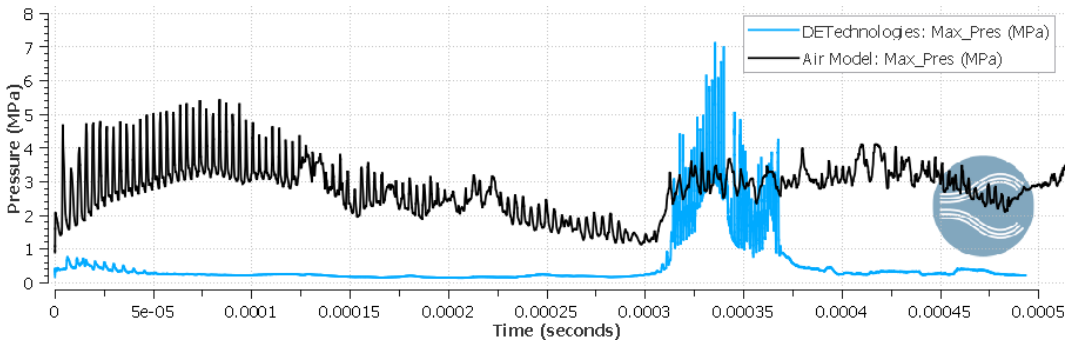

Figure 10: Comparison of Maximum Pressure of DETechnologies Model with Provided Model [33]

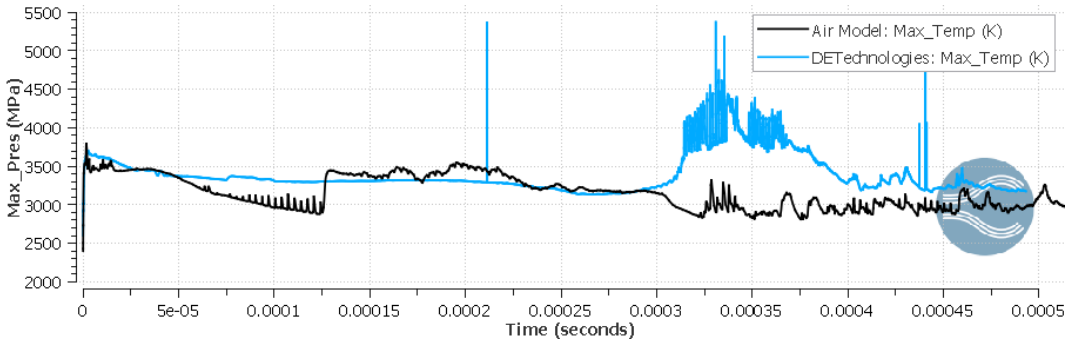

Figure 11: Comparison of Maximum Temperature of DETechnologies Model with Provided Model [33]

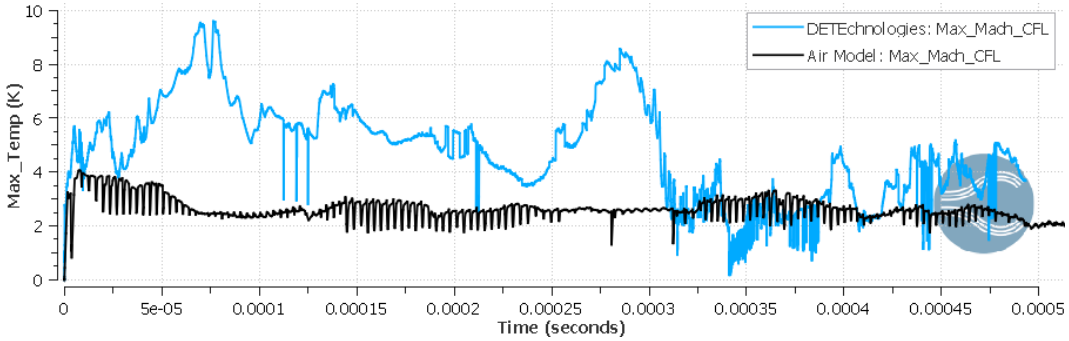

Figure 12: Comparison of Maximum Mach Number of DETechnologies Model with Provided Model [33]

The above gures (Figure 10, 11, 12) provide a crude comparison between current progress in DE-Technologies RDE model and the baseline air-hydrogen model provided in partnership with Convergent Science. The information seen above is not nal and does not provide a holistic snapshot of current CFD work, however, it is useful to illustrate the large inaccuracies found in the DETechnologies model by way of pressure spike, and Mach number. Work will continue to further develop this CFD model while validating results against published RDE data.

3.2.3 Structural Analysis

To date, structural analysis has been focused on the validation of su cient wall thickness in the RDE combustion chamber. Following engine geometry validation, the majority of the structural analysis will move away from hand calculations, and be focused in FEA - analyzing the structure reactions at operating frequencies, and the expected lifespan of the engine assembly due to combined loading and thermal fatigue e ects.

Due to the recent discovery of engine parameter resizing, the following analysis has been conducted using old engine parameters, and pending engine parameter validation, will be re-calculated to validate engine safety. The parameters used in this analysis are found below, in Table 11.

Table 11: Engine Parameters

Parameter	Value	Units
Maximum Pressure	4.30	MPa
Outer Diameter	55.11	mm
Inner Diameter	45.71	mm

The below properties, sourced from the ASM International handbook, assume the specimen is tested at an ambient temperature of 20°C. [34]

Table 12: Mechanical Properties of 316 Stainless Steel [34][35]

Property	Value	Units
Density	8.00	g/cc
Tensile Strength (Ultimate)	550	MPa
Tensile Strength (Yield)	240	MPa
Elongation at Break	60%	
Modulus of Elasticity	193	GPa
Poisson's Ratio	0.298	

The following theory is taken from Shigley's Mechanical Engineering Design [36]. The subsequent theory uses the following nomenclature:

Table 13: Pressure Vessel Stress Analysis Nomenclature [36]

Symbol	Name
$_t$	Tangential Stress
$_r$	Radial Stress
p_i	Internal Pressure
r_o	Outer Radius
r_i	Inner Radius

The assumption used in thick wall vessels is such that the longitudinal elongation is constant around the circumference of the cylinder - meaning the cross-section of the cylinder remains plane after loading. In cases where there is no external pressure acting on the vessel, the tangential and radial stresses can be calculated using the following equations:

$$_t = \frac{r_i^2 p_i}{r_o^2 \quad r_i^2}(1 + \frac{r_o^2}{r^2}) \tag{9}$$

$$_r = \frac{r_i^2 p_i}{r_o^2 \quad r_i^2}(1 \quad \frac{r_o^2}{r^2}) \tag{10}$$

Analyzing the stress due to internal pressure through the thickness, it is clear to understand that the maximum tangential and radial stresses occur at the inner radius, resulting in a maximum tangential stress (($_t)_{max}$) of 23.26 MPa, and a maximum radial stress (($_r)_{max}$) of 4.30 MPa. The factor of safety against yielding is therefore 10.32.

Table 14: Summary of Pressure Vessel Analysis

Metric	Value
$(_t)_{max}$	23.26 MPa
$(_r)_{max}$	4.30 MPa
FOS	10.32

Although this analysis validates the combustion chamber geometry, further structural analysis, using FEA, of the overall engine will be conducted before the final design. As previously discussed, this includes a modal analysis to understand engine behaviour near operating frequency, as well as a multi-physics fatigue analysis to understand maximum engine runtime due to combined loading and thermal stress effects.

3.2.4 Data Collection

Fuel and oxidizer plenum pressures and temperatures are often measured in test RDE's using K-type thermocouples and piezoelectric pressure transducers. Piezoelectric pressure transducers are used because of their high frequencies and ability to measure dynamic pressure fluctuations which makes detecting the rotating detonation wave position possible [37]. Figure 13 from Journell [37] demonstrates this phenomenon where the pressure spikes represent the rotating detonation wave passing over the pressure transducer location. Capillary Tube Average Pressure (CTAP) transducers are also used along the length of the combustion chamber to record an average pressure in the combustion chamber [38]. Recording the transient pressure response in the combustion chamber is difficult and expensive due to the high temperatures in the combustion chamber. When transient response or piezoelectric pressure transducers are flush mounted inside of the combustion chamber they are destroyed by the heat from the combustion process [38].

The RDE being designed for this project is designed to accommodate piezoelectric pressure transducers for measuring the pressures in the fuel and oxidizer plenums as well as one CTAP 12mm away from the combustion front inside of the combustion chamber. The RDE will also be able to accommodate K-type thermocouples for measuring fuel and oxidizer plenum temperatures as well as accommodating thermocouples to be mounted on the exterior surface of the outer body of the RDE. The RDE will be able to accommodate the pressure transducers and thermocouples but procurement and installation of them is out of scope for this capstone project due to their high cost and long lead times.

Figure 13: Pressure Spikes Indicating Rotating Detonation Wave Position [37]

3.2.5 Propellant Supply System

The following propellant supply system design is considered out of the scope of the capstone project due to cost, complexity, and insufficient lab space and resources for safe and professional operation. This design was built as a compilation of existing published literature to quantitatively analyze the compressible fluid flow from propellant storage tanks to the engine, such that a model could be developed that feeds stagnation conditions and mass flow rate, based on a specific feed system, into the analytical model. Inversely, the optimal desired stagnation and mass flow rate for engine performance could be used to back-calculate specific parameters like pipe diameter and length to determine or

validate if a feed system will work for an engine design. These functionalities will further re ne the analytical model outputs to be more accurate estimations of lab performance.

The basis for this P&ID is borrowed from similar engines operating on gaseous fuels that are available publicly. Good reviews of public RDE P&ID are provided by Mundt [5], Russo [24], Zhou [39], Andrus [40], Burke [41], Shank [42], Ma [43], Ishihara [44], and Goto [45].

At a high level, the gaseous oxygen and gaseous hydrogen are supplied separately by fuel tanks on site. The propellants ow from the supply tank through a pressure regulator, sonic nozzle, fast actuating valve, and check valve respectively until they reach the respective fuel and oxidizer plenum in the RDE. The fuel and oxidizer lines also branch o from their main lines to supply fuel and oxidizer to the DDTT. The pressure regulator is used in conjunction with the sonic nozzle to choke the uid ow and control the mass ow rate as supported by Equation 11 from John [46] where P_o is the upstream stagnation pressure. Pressure transducers are used directly upstream and downstream of the sonic nozzles to ensure a choked ow condition. Pressure transducers are also used directly upstream of the fuel and oxidizer inlets to measure stagnation pressure directly before the RDE, which can be used to calculate the initial conditions the RDE is receiving during the experiment.

Mass Flow Rate.

$$\underline{m} = \rho \frac{P_o}{RT_o} A \sqrt{\gamma} M \left(1 + \frac{1}{2} M^2\right)^{\frac{+1}{2(\quad 1)}} \tag{11}$$

Figure 14: Preliminary Piping and Instrumentation Diagram

Through collaboration with Swagelok Atlantic Canada representatives, the basics of this propellant supply system have been validated at a high level. Initial quotes to source most of this system from Swagelok are outlined in Table 15.

Collaborating with Sean Connolly-Boutin also yielded a design review of our P&ID which validated it as being well designed. Part of his graduate studies at Concordia University saw him design and implement a propellant feed system in his supervisor's (Dr. Charles Kiyanda) lab. The primary feedback on the system was regarding our supply tanks. Due to the very small ori ce at the top of standard compressed gas cylinders, the ow rate that is achievable with these tanks is very low, unless many are connected together with a manifold. The method that was developed for Concordia has a large ori ce o -the-shelf compressed gas cylinders functioning as the feed tank, with standard gas cylinders teed o the main feed line to be used to ll that feed tank.

Table 15: Initial Swagelok Bill of Materials

Item	Quantity	Price	Total Price
Tubing	25	$21.18	$529.50
Ori ce Plate	2	$707.88	$1,415.76
Ball Valve	5	$910.79	$4,553.95
Ball Valve Fitting	5	$322.65	$1,613.25
Check Valve	4	$449.21	$1,796.84
Union Fitting	4	$193.55	$774.20
Regulator	2	$1,330.71	$2,661.42
Female Fitting	5	$191.40	$957.00
Cross Union	10	$443.15	$4,431.50
		Extra Cleaning	$1,000.00
		Total	$19,733.42
		Tax	$2,960.01
		Grand Total	$22,693.43

3.2.6 Design For Manufacturing and Assembly

The appropriate tolerance analysis including GD&T is underway for part-level and assembly-level radial and axial tolerance stacks. The complete tolerance analysis will ensure the applied GD&T strategy is e ective for a functional RDE. A functional RDE has minimal total runout between the center body and outer body, the two surfaces that make up the annular chamber. A concentric annual chamber is crucial to an e ective operating RDE. Injector alignment is also of utmost importance for a functional RDE. Proper injector alignment will ensure su cient mixing in the combustion chamber between the fuel and oxidizer, as well as delivering the necessary mass ow rate, enabling the RDE to achieve detonation as well as aid the direction of the rotating detonation wave.

Injector alignment and the concentricity of the annular combustion chamber will be withheld to acceptable standards through proper communication through mechanical part and assembly drawings utilizing GD&T, communication with the machinist, and properly speci ed manufacturing and machining techniques.

4 Conclusion

This report summarizes the mid-term progress of the DETechnologies capstone team working towards Research and Development of a small scale Rotating Detonation Engine. Lack of published literature regarding a process for sizing a Rotating Detonation Engine has created a gap identi ed by the team as the interest area to focus on adding value with this project. Thus, e ort was put into developing a strong understanding of the rst-principles application of detonation theory, approaching the design from a theoretical (analytical) angle. To direct the design scope and provide model validation, a small-scale Rotating Detonation Engine is to be designed to match the design point of a well-tested pre-existing engine system with the intent of producing a hot- reable prototype. Objectives for the design are a thrust output of 1350N, using a gaseous non-premixed Hydrogen and Oxygen propellant.

The preliminary analytical model sizes an engine to operate at 180 kPa stagnation pressure, at an equivalence ratio of 1. The engine combustion chamber is tentatively sized with an outer diameter of 36.8mm and annular channel width of 3.128mm. Performance predictions are that this geometry will produce 1350N of thrust, with a speci c impulse of 414.7s ^{1}, and require a supplied mass ow rate of between 32.8$\frac{g}{s}$ and 65.1 $\frac{g}{s}$. Wave speed within the combustion chamber is expected to be 2.86$\frac{km}{s}$, with a maximum expected pressure of 6.03 MPa, and temperature of 3783K.

A recent discovery of an error in early implementations of the analytical calculations has set back the timeline for downstream engineering design work. Previous results, shown for a similar, but slightly larger engine design are presented. Combustion Computational Fluid Dynamics e orts are underway to validate analytical predictions of constrained detonation within the Rotating Detonation Engine combustion chamber. The current status of combustion Computational Fluid Dynamics conversion of a provided Hydrogen and Air combustion mode to Hydrogen and Oxygen is presented in brief. Structural analysis for the Rotating Detonation Engine combustion chamber as a thick-walled pressure

vessel shows that the current design concludes a Factor of Safety of 10.32. The high Factor of Safety is typical for this industry due to the very unpredictable nature of detonation.

Theoretical Piping and Instrumentation Diagram for a propellant supply system are presented to guide nal engine design. Works towards preparing the engine for fabrication are presented along with the plan for conducting formal Geometric Dimensioning and Tolerancing analysis to ensure manufacturing accuracy.

Acronyms

BOM	Bill of Materials 20, II
CAD	Computer Aided Design 8
CalTech	California Institute of Technology 10
CFD	Computational Fluid Dynamics 8{10, 15, 16, 20, I
CJ	Chapman Jouguet 13, 14
CTAP	Capillary Tube Average Pressure 18
DDTT	De agration-to-Detonation Transition Tube 19
DFMA	Design For Manufacturing and Assembly 8, 10, 20, I
FEA	Finite Element Analysis 9, 16, 18, I
FOS	Factor of Safety 21
GD&T	Geometric Dimensioning and Tolerancing 8, 20, 21
P&ID	Piping and Instrumentation Diagram 19, 21, II
PDE	Pulse Detonation Engine 3, 28
PMP	Project Management Plan 7, 8
R&D	Research and Development 20
RDE	Rotating Detonation Engine 1{3, 5{7, 10, 13{16, 18{20, 26{28, I, II
ZND	Zel'dovich, von Neumann and Doring 13

References

[1] I. J. Shaw, J. A. Kildare, M. J. Evans, A. Chinnici, C. A. Sparks, S. N. Rubaiyat, R. C. Chin, and P. R. Medwell, \A theoretical review of rotating detonation engines," Direct Numerical Simulations-An Introduction and Applications , 2019.

[2] B. V. Voitsekhovskii, \Detonation combustion of a gas mixture in a cylindrical chamber," Doklady Akademii Nauk SSSR, vol. 129, no. 6, 1959.

[3] F. A. Bykovskii and V. V. Mitrofanov, \Detonation combustion of a gas mixture in a cylindrical chamber," Combustion, Explosion and Shock Waves, vol. 16, pp. 570{578, Sept. 1980.

[4] S. F. Connolly-Boutin, Detonation Physics-Based Modelling & Design of a Rotating Detonation Engine. PhD thesis, Concordia University, 2019.

[5] T. Mundt, Geometric Scaling of Cylindrical Rotating Detonation Rocket Engine Combustors. PhD thesis, 2023.

[6] S. A. Zhdan, F. A. Bykovskii, and E. F. Vedernikov, \Mathematical modeling of a rotating detonation wave in a hydrogen-oxygen mixture," Combustion, explosion, and shock waves, vol. 43, pp. 449{459, 2007.

[7] F. A. Bykovskii, S. A. Zhdan, and E. F. Vedernikov, \Continuous spin detonations," Journal of propulsion and power, vol. 22, no. 6, pp. 1204{1216, 2006.

[8] M. L. Fotia, F. Schauer, T. Kaemming, and J. Hoke, \Experimental study of the performance of a rotating detonation engine with nozzle," Journal of Propulsion and Power, vol. 32, no. 3, pp. 674{681, 2016.

[9] J. Kindracki, P. Wolanski, and Z. Gut, \Experimental research on the rotating detonation in gaseous fuels{oxygen mixtures," Shock waves, vol. 21, pp. 75{84, 2011.

[10] K. K. Kuo, \Principles of combustion," 1986.

[11] P. Wolanski, \Detonative propulsion," Proceedings of the combustion Institute, vol. 34, no. 1, pp. 125{158, 2013.

[12] F. A. Bykovskii and V. Mitrofanov, \Detonation combustion of a gas mixture in a cylindrical chamber," Combustion, Explosion and Shock Waves, vol. 16, no. 5, pp. 570{578, 1980.

[13] D. L. Chapman, \Vi. on the rate of explosion in gases," The London, Edinburgh, and Dublin Philosophical Magazine and Journal of Science, vol. 47, no. 284, pp. 90{104, 1899.

[14] E. Jouguet, \Sur la propagation des reactions chimiques dans les gaz [on the propagation of chemical reactions in gases]," Journal de Mathematiques Pures et Appliquees, vol. 60, p. 345, 1905.

[15] C. A. Nordeen, \Thermodynamics of a rotating detonation engine," 2013.

[16] S. J. Miller, \Design and testing of an h2/o2 predetonator for a simulated rotating detonation engine channel," 2013.

[17] S. R. Chakravarthy, \Mod-06 lec-26 velocity, temperature and entropy variation along hugoniot curve," Jun 2016.

[18] Y. B. Zel'dovich, \ [on the theory of the propagation of detonation in gaseous systems]," Journal of Experimental and Theoretical Physics, vol. 10, pp. 542{568, 1940.

[19] J. von Neumann, \Theory of detonation waves," tech. rep., Institute for Advanced Study, 1942.

[20] W. Doring, \Uber den detonationsvorgang in gasen [on the detonation process in gases]," Annalen der Physik, vol. 435, pp. 421{436, 1943.

[21] A. Gavrikov, A. E menko, and S. Dorofeev, \A model for detonation cell size prediction from chemical kinetics," Combustion and ame, vol. 120, no. 1-2, pp. 19{33, 2000.

[22] H. D. Ng, Y. Ju, and J. H. Lee, \Assessment of detonation hazards in high-pressure hydrogen storage from chemical sensitivity analysis," International Journal of Hydrogen Energy, vol. 32, no. 1, pp. 93{99, 2007.

[23] C. K. Westbrook and P. A. Urtiew, \Use of chemical kinetics to predict critical parameters of gaseous detonations," Combustion, Explosion and Shock Waves, vol. 19, no. 6, pp. 753{766, 1983.

[24] R. M. Russo, \Operational characteristics of a rotating detonation engine using hydrogen and air," 2011.

[25] A. P. Nair, A. R. Keller, N. Q. Minesi, D. I. Pineda, and R. M. Spearrin, \Detonation cell size of liquid hypergolic propellants: Estimation from a non-premixed combustor," Proceedings of the Combustion Institute, vol. 39, no. 3, pp. 2757{2765, 2023.

[26] J. W. Bennewitz, J. R. Burr, B. R. Bigler, R. F. Burke, A. Lemcher , T. Mundt, T. Rezzag, E. W. Plaehn, J. Sosa, I. V. Walters, et al., \Experimental validation of rotating detonation for rocket propulsion," Scienti c Reports , vol. 13, no. 1, p. 14204, 2023.

[27] R. Burke, \Rotating detonation engine injector and method of designing," U.S. Patent 2023/0340931 A1, Oct. 2023.

[28] P. Wolanski, \Detonation rocket engine comprising an aerospike nozzle and centring elements with cooling channels," U.S. Patent 11,795,891 B2, Oct. 2023.

[29] S. Miri, L. Palmer, A. Clark, and P. Cleary, \Report three: Final term report - detechnologies - rotating detonation engine," Aug 2023.

[30] S. Connolly-Boutin, V. Joseph, H. Ng, and C. Kiyanda, \Small-size rotating detonation engine: scaling and minimum mass ow rate," Shock Waves, vol. 31, no. 7, pp. 665{674, 2021.

[31] M. Kaneshige and J. E. Shepherd, \Detonation database," 1997.

[32] J. E. Shepherd and J. Kasahara, \Analytical models for the thrust of a rotating detonation engine," 2017.

[33] K. J. Richards, P. K. Senecal, and E. Pomraning, \Converge 3.19," 2024.

[34] S. Washko and G. Aggen, \Wrought Stainless Steels," in Properties and Selection: Irons, Steels, and High-Performance Alloys, ASM International, 01 1990.

[35] \316 stainless steel, annealed bar." https://www.matweb.com/search/DataSheet.aspx?MatGUID=dfced4f11d63459e8ef8733d1c7c1ad2&ckck=1 Accessed: 2023-01-16.

[36] R. Budynas, Shigley's Mechanical Engineering Design McGraw-Hill series in mechanical engineering, McGraw-Hill Higher Education, 2014.

[37] C. L. Journell, R. M. Gejji, I. V. Walters, A. I. Lemcher , C. D. Slabaugh, and J. B. Stout, \High-speed diagnostics in a natural gas{air rotating detonation engine," Journal of Propulsion and Power, vol. 36, no. 4, pp. 498{507, 2020.

[38] C. A. Stevens, M. Fotia, J. Hoke, and F. Schauer, \Comparison of transient response of pressure measurement techniques with application to detonation waves," in 53rd AIAA Aerospace Sciences Meeting, p. 1102, 2015.

[39] S. Zhou, Y. Ma, F. Liu, and N. Hu, \Experimental investigation on pulse operation characteristics of rotating detonation rocket engine," Fuel, vol. 354, p. 129408, 2023.

[40] I. Q. Andrus, \A premixed rotating detonation engine: Design and experimentation," AIR FORCE INSTITUTE OF TECHNOLOGY WRIGHT-PATTERSON AFB OH WRIGHT-PATTERSON , 2016.

[41] R. Burke, Characteristics of Rotating Detonation Engines for Propulsion and Power Generation. PhD thesis, University of Central Florida, 2022.

[42] J. C. Shank, "Development and testing of a rotating detonation engine run on hydrogen and air," 2012.

[43] J. Z. Ma, S. Zhang, M. Luan, and J. Wang, "Experimental investigation on delay time phenomenon in rotating detonation engine," Aerospace Science and Technology, vol. 88, pp. 395–404, 2019.

[44] K. Ishihara, Y. Kato, K. Matsuoka, J. Kasahara, A. Matsuo, and I. Funaki, "Thrust performance evaluation of a rotating detonation engine with a conical plug," in 25th International Colloquium on the Dynamics of Explosions and Reactive Systems, Leeds, UK, 2015.

[45] K. Goto, Y. Kato, K. Ishihara, K. Matsuoka, J. Kasahara, A. Matsuo, I. Funaki, D. Nakata, K. Higashino, and N. Tanatsugu, "Thrust validation of rotating detonation engine system by moving rocket sled test," Journal of Propulsion and Power, vol. 37, no. 3, pp. 419–425, 2021.

[46] J. John and T. Keith, Gas Dynamics. Pearson Prentice Hall, 2006.

[47] C. B. Greene, J. M. Donohue, and P. A. T. Cocks, "Regenerative cooling and adjustable throat for rotating detonation engine," U.S. Patent 11,852,077 B2, Dec. 2023.

[48] Q. Liu and L. Qiao, "Injection manifold with tesla valves for rotating detonation engines," U.S. Patent 11,767,979 B2, Sep. 2023.

[49] E. J. Gutmark, V. A. Anand, A. St. George, W. Stoddard, and E. Knight, "Rotating detonation engines and related devices and methods," U.S. Patent 11,761,635 B2, Sep. 2023.

[50] A. R. Mizener and F. K. Lu, "Systems, apparatuses and methods for improved rotating detonation engines," U.S. Patent 11,592,183 B2, Feb. 2023.

A Additional United States Patents

A.1 Regenerative Cooling and Adjustable Throat for Rotating Detonation Engine

The United States patent US 11,852,077 B2 [47] is entitled "Regenerative Cooling and Adjustable Throat for Rotating Detonation Engine" and was published by Christopher Britton Greene of Raytheon Technologies Corporation.

The patent comprises a method of operating a rotating detonation using regenerative cooling and heated liquid fuel. The following, are the claims included in this patent:

1. The RDE operates using a owing liquid on at least one inner and outer wall, in addition to a heated liquid fuel owing to a mixer at the inlet. The additional fuel is fed to an injector on the annular wall of the engine - where the detonation occurs in the annular detonation chamber.
2. The "heated liquid fuel" is super-heated
3. The detonation induces a rotating wave around the circumference of the annular detonation chamber.
4. Liquid phase fuel ows along the outer wall.
5. Liquid phase fuel ows along the outer and inner walls.
6. The liquid fuel maintains the pressure of the heated liquid to ensure the heated liquid remains liquid.
7. The outlet is de ned such as the area between the static engine and movable ow wherein the movable ow restriction can move relative to the static structure.
8. Flow happens at conditions su cient to allow fuel to change from liquid to gas.
9. Fuel temperature and pressure drop must occur in at least one fuel injector.
10. Fuel is considered to be aviation fuel.
11. Oxidizer is fed to detonation chamber through at least one fuel injector.
12. Flowing liquid to the mixer involves owing fuel through at least one fuel injector.
13. At least one fuel injector is downstream of an oxidizer inlet.
14. At least one fuel injector is upstream of an oxidizer inlet.
15. The heated liquid fuel ows through at least one fuel injector arranged at an angle.

A.2 Injection Manifold with Tesla Valves for Rotating Detonation Engines

The United States patent US 11,767,979 B2 [48] is entitled "Injection Manifold with Tesla Valves for Rotating Detonation Engines" and was published by Qili Liu of the Purdue Research Foundation.

This patent explores the design of an RDE featuring Tesla valves to eliminate the potential of reverse gas ow into the fuel or oxidizer manifold. Below, are the claims included in the patent:

1. The RDE includes an injector assembly, fuel manifold, oxidizer manifold, and combustion chamber, where the injector assembly includes Tesla valves for both the fuel and oxidizer.
2. The Tesla valve is de ned as a valve with a loop-shape nishing in elongated ends.
3. The Tesla valves are aligned in a parallel-aligned orientation, meaning the fuel and oxidizer injectors form a parallel-aligned orientation.
4. The valves are arranged into pairs found at 90.
5. The injection assembly parts are manufactured using additive manufacturing methods.

6. The injectors are made from a group of materials including stainless steel, INCONEL®, titanium alloys and ceramics.
7. The RDE injector includes an inner body, outer body forming a cylindrical annulus.
8. The cylindrical annulus of the RDE is forms the fuel and oxidizer manifold.
9. The Tesla valves terminate in an injector found on the inner surface of the cylindrical body.
10. The Tesla valves have a characteristic length of 20 mm, with a diameter of 1 mm. Back- ow is prevented if the pressure ratio between combustion chamber and injection manifold is between 5 and 35.
11. Reverse ow is prevented using a rst and second chamber, in addition to multiple Tesla valves.
12. The rst chamber is the fuel manifold, and the second chamber is the oxidizer manifold - and the two meet in the combustion chamber, where detonation begins.
13. The Tesla valves are formed of loop-shapes forming an o set gure-eight to prevent back- ow.
14. The reverse ow prevention of parallel-aligned, where alternating fuel and oxidizer ports are misaligned, aligned series at an angle with respect to one another.
15. The reverse ow con guration uses Tesla valves in a 90° arrangement.
16. The Tesla valves are manufactured using additive manufacturing.
17. All Tesla valves are manufactured from a group of materials including stainless steel, INCONEL®, titanium alloys and ceramics.
18. The reverse ow relies on a characteristic valve length of 20 mm with a diameter of 1 mm with the pressure ratio between 5 and 35.

A.3 Rotating Detonation Engines and Related Devices and Methods

The United States patent US 11,761,635 B2 [49] is entitled "Rotating Detonation Engines and Related Devices and Methods" and was published by Ephraim J. Gutmark of the University of Cincinnati.

This patent explores the design of a non-premixed RDE. Key claims made in this patent are:

1. The rotating detonation combustor contains an outer shell and base which act to de ne the combustion chamber, with a longitudinal axis - where the exhaust outlet is concentric to this axis.
2. Nozzle is removably coupled to the body.
3. The combustion expands radially outward towards the exhaust opening.
4. The detonation chamber is ared.
5. The nozzle is connected to the combustor which chokes the exhaust opening.
6. The nozzle is comprised of a nozzle inlet and outlet, and a converging surface found between the nozzle inlet and outlet.
7. The RDE nozzle de nes the front between outer surface and converging end of the nozzle.
8. The RDE combustor includes at least one ramping surface on the outer edge of the combustion chamber.
9. There is at least one obstruction found along the outer edge of the combustion chamber.

A.4 Systems, Apparatuses and Methods for Improved Rotating Detonation Engines

The United States patent US 11,592,183 B2 [50] is entitled "Systems, Apparatuses and Methods for Improved Rotating Detonation Engines" and was published by Andrew R. Mizener of the University of Texas.

This patent explores a typical RDE design in addition to a premix chamber, and injection swirl. Key claims included in this patent are:

1. The RDE is comprised of an outer body, inner body and annular gap. In addition to the main geometry, cooling circulates within the inner and outer bodies to provide cooling throughout the engine.
2. The injectors are positioned at an angle between 0 - 90° relative to the centre longitudinal axis of the engine.
3. The injection ports are either straight, contoured converging-diverging or conical converging-diverging.
4. The outer housing of the RDE connect to inlet and outlet cooling hoses to provide additional cooling to the engine.
5. The head of the engine includes a mixing chamber prior to the injectors.
6. The mixing chamber is an annular recess within the head of the engine.
7. The injection plate is found between the mixing chamber and annular combustion chamber.
8. An end cap connects the inner and outer caps.
9. The inner shell connects to the end cap with mounting legs.
10. The gaps between the legs of the inner shell form cooling channels.
11. There is an igniter connected to the cylindrical outer body.
12. The igniter takes the form of a Pulse Detonation Engine (PDE).